Optimization of Silver Ion Concentration into the Lattice of Zinc Oxide Nanoparticles Synthesized via a Hydrothermal Approach

E. O. Ojegu[1], R. A. Daniel-Umeri[2], E. C. Nwaokorongwu[3], Nawal Alghamdi[4,] I. L. Ikhioya[5, 6*]

[1]Department of Physics, Delta State University, Abraka. Delta State, Nigeria
[2]Department of Physics, Delta State University of Science and Technology, Ozoro. Delta State, Nigeria.
[3]Department of Physics, College of Physical and Applied Sciences, Michael Okpara University of Agriculture, Umudike, Abia State, Nigeria.
[4]Department of Physics, Faculty of Science, University of Tabuk, Tabuk, Saudi Arabia
[5]Department of Physics and Astronomy, University of Nigeria, Nsukka, Enugu State, Nigeria
[6]Department of Physics, Federal University, Lokoja, Kogi State, Nigeria.

Abstract: The exceptional properties of Ag-doped ZnO nanoparticles (NPs) make them highly promising for applications in environmental remediation and optoelectronics. However, the limited tunability of ZnO's bandgap and its suboptimal performance in doping applications necessitates material modifications. In this study, a hydrothermal method was used to synthesize ZnO and Ag-doped ZnO (NPs). The study optimized the silver molar concentration to between 0.01 to 0.03 mol and characterized the nanoparticles for their optical, structural, and surface micrograph using different characterization techniques. As the wavelength increases from 300 to 1100 nm, nanoparticles show a decrease in absorbance. In both spectral regions, ZnO doped with 0.1 mol of Ag exhibited the highest absorbance, while ZnO doped with 0.2 mol of Ag showed the lowest absorbance. The energy bandgap of ZnO was measured at 2.19 eV, which deviates from the theoretical bandgap of ZnO at 3.3 eV. Introducing silver into the ZnO leads to changes in the band structure because of the creation of additional energy levels while the introduction of silver doping into ZnO lattice leads to a decrease in the bandgap energy to 1.50, 1.39, and 1.29 eV. These enabled electron transitions at lower energy levels because of the formation of defect states or interaction with ZnO. The XRD patterns of zinc oxide and Ag-doped ZnO NPs reflect their hexagonal structure. The material showed a diffraction peak at (101) when measured at a 2θ angle of 44.863°. The hexagonal phase displayed distinct diffraction peaks at specific 2θ angles. Within the FTIR spectrum, Zn-O stretching vibrations are typically shown by distinct absorption bands, usually ranging from 400 to 750 $cm^{-1.}$ Introducing silver doping results in the emergence of new vibrational modes and a shift in existing peaks which indicate changes in the local environment around the ZnO lattice. These findings demonstrate that silver doping significantly enhances the optical and structural properties of ZnO an indication of its suitability for applications in advanced technologies requiring tunable bandgap and improved performance.

Keywords: *Hydrothermal, Nanoparticles, bandgap, Zinc Oxide, Nanometer*

[Received Sep. 27, 2024; Revised Oct. 24, 2024; Accepted Nov 6, 2024] Print ISSN: 0189-9546 | Online ISSN: 2437-2110

I. INTRODUCTION

Nano-scale materials are synthesized using different approaches in various scientific domains where nanotechnology is applied. Nanoparticles are small particles that form nanomaterials. The crucial magnetic, electrical, and optical properties of nanoparticles have led to their widespread use in the advancement of multiple industries, including optics, sensing, data storage communications, energy storage, transmission, cosmetics, environmental protection, and biology (Malik *et al.*, 2015). Nanoparticles exhibit unique properties and utility because they share a similar size with biomolecules. Various metals and semiconductor core materials can create nanoparticles, giving them beneficial properties such as fluorescence and magnetism (Lakshmipriya and

*Corresponding author: imosobomeh.ikhioya@unn.edu.ng
doi: http://dx.doi.org/10.4314/njtd.v21i4.2933

Gopinath, 2020). Nanoparticles exhibit decreased size in contrast to bulk materials, resulting in higher surface areas and volume ratios as size decreases. Decreasing the particle size results in higher reactivity and distinct physical properties because of the increased number of atoms near the particle surface. Nanoparticles made of specific materials exhibit unique material properties (Chandrasekar *et al.*, 2019). Therefore, mechanistic methods are necessary to manipulate and control these properties (Dhoke, 2023). The main challenge in nanoparticle growth is creating nanomaterials of consistent size and shape through simple synthesis methods. Scientists have spent the past decade developing methods to control the micrograph and size of nanoparticles precisely. Chemical methods are commonly used in nanoparticle synthesis due to their cost-effectiveness, reliability, and environmental friendliness. In addition, they offer the ability to precisely manipulate the shape and size of nanoparticles (Strachowski *et al.*, 2022). The primary problem occurs when tiny particles in the solution clump together, as nanoparticles with a high surface-to-volume ratio are needed without any stabilizer. The growth of nanoparticles requires stable colloids. Steric repulsion is created by surfactants, polymers, or organic molecules on the nanoparticle surface, which stabilizes the nanoparticles (Aravind *et al.*, 2013). Van der Waals repulsion can also influence nanoparticle stabilization. The literature contains reports of different NPs, such as metal-metal oxide NPs, and polymer NPs, because of phase separation and poor dispersion can arise during synthesis, complicating their application. The diverse properties and functionalities of metal-oxide NPs make them stand out as highly versatile materials (Maher *et al.*, 2023; Widiyandari *et al.*, 2023). Zinc-oxide (ZnO) NPs are important among different metal-oxide NPs because of their extensive application (Król *et al.*, 2017) in gas sensors, storage, chemical sensors, optical, bio-sensors, solar cells, cosmetics, electrical devices, and drug-delivery (Mohan *et al.*, 2020). With its wide band gap of 3.37 eV, strong bonding, and high exciton binding energy 60 meV at room temperature, ZnO is highly sought-after for short-wavelength optoelectronics. Solid-state optoelectronics for blue to ultraviolet (UV) light, such as laser advancements, utilize ZnO, a wide band gap material (Khudiar, Mutlak and Nayef, 2021). The non-centrosymmetric crystal structure of ZnO enables it to display piezoelectric properties, making it useful in the development of sensors and actuators.

The hydrothermal approach was employed by (Mohan *et al.*, 2020) to prepared Zinc Oxide (ZnO) nanoparticles, and the resulting properties were examined. The presence of ZnO bonding and the purity of the materials were verified using FTIR studies. The size of the grain decreased with higher reaction temperatures and increased with longer reaction times. Nanorods are generated at the same reaction temperature according to TEM images, while different temperatures result in the observation of nanoflowers and nanosphere. Changes in inter-planar spacing in UV-vis cause variations in the intensity of luminescence peaks. The change in bandgap value is a result of the difference in nanoparticle size. The Sol-gel method, as reported by (Hasnidawani *et al.*, 2016), allows for precise control of particle size and morphology through systematic monitoring of reaction parameters. According to the EDX analysis, the ZnO NPs are highly pure, containing 55.38% zinc. The XRD spectrum shows prominent peaks for oxygen and zinc, indicating their crystalline nature. A rod-like structure is observed in the synthesized ZnO, as shown by FESEM micrographs. The ZnO nanoparticles obtained are uniform in size and show good crystallinity, as confirmed by the XRD result. ZnO nanoparticles were effectively synthesized using the sol-gel method, achieving sizes of 81.28 nm and 84.98 nm. (Zhou *et al.*, 2023) highlighted the use of zinc oxide nanoparticles ZnO NPs in agriculture and the food industry to control microorganisms. The direct effect of ZnO NPs' antibacterial properties on human health may lead to improved food quality. Zinc oxide nanoparticles (ZnO NPs), extensively researched inorganic nanoparticles, are generating attention and interest in agriculture and food sectors. According to **(Primo *et al.*, 2020),** zinc oxide NPs were successfully synthesized using Aloe vera and Cassava starch through two straightforward methods. XRD patterns and Raman spectra confirmed single-phase ZnO in both cases. Zinc atoms in the Zn^{2+} oxidation state is detected in the XPS results. Cassava starch synthesis of ZnO nanoparticles showed pseudo-spherical nanoparticles and nano sheets in SEM images. The synthesis of Aloe vera only produced pseudo-spherical nanoparticles. A slight discrepancy was observed in the absorption edge of ZnO particles in the UV-Vis spectra when Aloe vera 3.18 eV and Cassava starch 3.24 eV were employed. The effectiveness of ZnO NPs as copper adsorbents in wastewater was tested. The results show that both synthesis methods have similar effectiveness in removing low concentrations of Cu^{2+} ions (~40 mg/L). Yet, when the concentration of the substance being absorbed goes beyond 80 mg/L, Aloe vera-synthesized ZnO nanoparticles show higher efficiency in removing it. The potential of the prepared ZnO NPs as efficient and eco-friendly metal trace absorbers in wastewater is high.

Although numerous studies have examined Ag-doped ZnO properties, the specific mechanisms underlying the influence of silver on ZnO's electronic and structural properties are not well understood. Further

investigation is necessary to understand these mechanisms at the atomic level. There is no agreement on the best silver concentration for desired properties. Various studies show different outcomes, and comprehensive research is necessary to establish optimal doping levels for specific uses. The stability of Ag-doped ZnO nanoparticles under different environmental conditions (e.g., UV exposure, temperature changes) has not been well-documented in the long term (Venkatasubramanian and Sundaraj, 2014; Rahmah *et al.*, 2023). Further research is necessary to evaluate their durability and possible degradation routes. Despite numerous attempts to explore synthesis techniques, the potential for industrial application scalability is not well understood (Venkatasubramanian and Sundaraj, 2014; Jothibas *et al.*, 2019; A and M, 2022; Hashem and El-Sayyad, 2023; Rahmah *et al.*, 2023). It is of great importance to study synthesis techniques that are both affordable and replicable. Despite the potential of Ag-doped ZnO nanoparticles in biomedicine, there is a lack of information on their compatibility and toxicity to human cells and the environment. Additional comprehensive studies are necessary to evaluate safety profiles. Most research focuses on general properties, but it's crucial to conduct application-specific studies to examine how Ag-doped ZnO performs in real-world situations like photocatalysis, sensors, or antimicrobial coatings. Research on incorporating Ag-doped ZnO nanoparticles into composite materials has been limited. The exploration of their synergistic effects, in combination with other materials, could pave the way for innovative applications (Venkatasubramanian and Sundaraj, 2014; Jothibas *et al.*, 2019; Hashem and El-Sayyad, 2023). By addressing these gaps, the understanding and potential use of Ag-doped ZnO nanoparticles can be enhanced in diverse fields.

Among different fabrication methods, the hydrothermal method stands out as a crucial technique for producing distinct ZnO shapes due to its ability to control crystallite growth and facilitate scaling up. The influence of capping molecules, kinetic barrier, temperature, and time on crystallization can be observed under non-equilibrium kinetic growth conditions. The rate of crystallization can be regulated by altering the temperature or pH of the reaction, allowing for a faster overcoming of the kinetic barrier (Aneesh, Vanaja and Jayaraj, 2007). The selection of salt can influence the synthesis course as the metal source for the metal oxide. Researchers need to conduct comprehensive studies to examine how hydrothermal synthesis parameters impact the morphology, size, and properties of Ag-doped ZnO nanoparticles. Although silver doping is studied, the molecular-level mechanisms of Ag ions interacting with ZnO during hydrothermal process remain unclear (Hashem and El-Sayyad, 2023). There is still limited research on the scalability of the hydrothermal method for industrial applications. Assessing the feasibility of large-scale production requires studies on reproducibility and cost-effectiveness. Although general properties have been investigated, there is a research gap regarding the performance of hydrothermally synthesized Ag-doped ZnO nanoparticles in specific applications.

By doping ZnO with Ag, the photocatalytic efficiency of ZnO can be improved, leading to enhanced charge separation and reduced electron-hole recombination. These qualities make them very efficient for tasks such as wastewater treatment and air purification (Rahmah *et al.*, 2023). The addition of silver improves the antibacterial properties of ZnO, making these nanoparticles valuable in medical applications, coatings, and packaging materials for preventing microbial growth. The optical properties of Ag-doped ZnO are exceptional, with a modified bandgap energy that can be tailored for specific applications in optoelectronics and sensors. The thermal and structural stability of ZnO nanoparticles can be enhanced by doping with silver, leading to improved performance in various environmental conditions (Jothibas *et al.*, 2019). The overall performance of silver and zinc oxide in applications, such as enhanced photocatalytic degradation of pollutants, can be improved through synergistic effects when they are combined (Widiyandari *et al.*, 2023). The exceptional properties of Ag-doped ZnO nanoparticles make them highly promising for applications in environmental remediation, healthcare, and electronics.

In this study, hydrothermal synthesis was used to produce ZnO and Ag-doped ZnO NPs. The nanoparticles underwent optical characterization using a UV-visible spectrophotometer, phase analysis using X-ray diffraction, surface micrograph using scanning electron microscopy, and the presence of metal oxide bonding and functional group was confirmed using FTIR.

II. MATERIALS AND METHODS

A. Materials

The chemical material used for preparing Ag doped zinc oxide NPs were obtained from Sigma Aldrich are; Silver nitrate $AgNO_3$ (98%), zinc nitrate hexahydrate $Zn(NO_3)_2.6H2O$ (99%), potassium Hydroxide (KOH) (99%), and distilled water. The chemicals employed were pure enough with no additional purification.

B. Hydrothermal preparation procedure of Ag doped zinc oxide NPs

In the synthesis of silver doped zinc oxide nanoparticles, 2.082 g of zinc nitrate hexahydrate $Zn(NO_3)_2.6H2O$ were dissolved in 35 mL of distilled water and stirred for 40 mins. 3.927 g of potassium hydroxide (KOH) was dissolved in 35 mL of distilled water and stirred for 40 minutes. The zinc nitrate hexahydrate was continuously stirred while adding drops of the potassium hydroxide precursor to achieve a pH level of 12. The mixture was stirred for 40 minutes. The balance precursor, which had a pH of 12, was placed into a Teflon lined autoclave and left in the hydrothermal oven for 3 hours at a temperature of 90°C. Then the Teflon was taken out of the oven and allowed to cool naturally to room temperature. The solution was centrifuge at 6000 rpm , then washed with distilled water 3 times and transferred the remaining particles into a crucible kept in the oven to dry. For the synthesis of silver doped zinc oxide nanoparticles, we adapted the same procedure. 0.0339 g of (0.1 mol) of silver nitrate were dissolved in 20 mL of distilled water separately. The combination of zinc nitrate hexahydrate and silver nitrate was stirred for 40 minutes. The zinc nitrate hexahydrate and silver nitrate were mixed and stirred constantly while gradually adding potassium hydroxide to achieve a pH level of 12. The stirring continued for 45 minutes. The precursor with a pH of 12 was put in a Teflon-lined autoclave and kept in the hydrothermal oven at 90°C for 3 hours. The Teflon was removed from the oven and left to cool down to room temperature. The solution underwent centrifugation at 6000 rpm, followed by three washes with distilled water. The remaining particles were then moved to a crucible and dried in the oven. The process was repeated for 0.679 g of (0.2 mol), and 0.1019 g of (0.3 mol) of silver nitrate to form silver doped zinc oxide nanoparticles. The obtained samples were labelled as ZnO_2, Ag $_{(0.1\ mol)}$/ ZnO_2, Ag $_{(0.2\ mol)}$/ ZnO_2, and Ag $_{(0.3\ mol)}$/ ZnO_2. Figure 1 illustrates the experiment. Using X-ray diffraction (Bruker D8 Advance), the structural analysis of the material was determined. The presence of metal oxide bonding and functional group was confirmed through FTIR analysis. The material's surface morphology was analyzed using scanning electron microscopy. The material's absorbance was measured using a UV visible spectrophotometer.

Figure 1: schematic diagram for the hydrothermal process of Ag doped zinc oxide NPs

III. RESULT AND DISCUSSIONS

A. Optical analysis of silver doped zinc oxide NPs

UV-Vis spectroscopy was used to measure the absorbance spectrum of Ag-doped zinc oxide NPs. The absorption rate of Ag-doped zinc oxide NPs, synthesized via a hydrothermal approach, is depicted in Figure 2 (a). The material displayed a permanent peak in absorbance in the visible region of the plot, suggesting absorption of the UV light spectrum. The absorbance of the nanoparticles decreases as the wavelength increases from 300 to 1100 nm. The highest absorbance in both spectral regions was observed in zinc oxide doped with 0.1 mol of silver, while the lowest absorbance was seen in zinc oxide doped with 0.2 mol of silver. Among all the materials, the material synthesized with 0.3 mol of silver exhibits a moderate absorbance. The absorbance of the materials aligns with the absorbance reported in the literature (Mohan *et al.*, 2020). The materials exhibit similar peaks, particularly at wavelengths of (650, 789, 948, 1067) nm, with corresponding absorbance values of (266, 234, 262, 253) (Mohan *et al.*, 2020; Khudiar, Mutlak and Nayef, 2021;

Strachowski *et al.*, 2022; Zhou *et al.*, 2023) respectively. Introducing silver ions changes the electronic structure of zinc oxide, enhancing its photocatalytic activity and altering its optical properties. The presence of plasmon resonance in silver nanoparticles results in increased light absorption via localized surface plasmon resonance (Malik *et al.*, 2015). This effect leads to a boost in the overall absorbance of the Ag-doped zinc oxide NPs. Peaks observed in the absorbance spectrum can identify specific electronic transitions. The absorbance changes with wavelength, frequently exhibiting higher absorbance in the UV region because of ZnO's inherent characteristics and the added effects of silver doping. Increased silver dopant concentrations result in moderate absorbance because of heightened light interactions. Absorbance is affected by the shape and size of the NPs, which influence surface area and light scattering (Malik *et al.*, 2015). The efficiency of photocatalytic reactions is improved by enhanced absorbance in the visible range, making Ag-doped zinc oxide NPs suitable for environmental remediation, photovoltaic, and solar cell applications. Sensors can use the optical properties to detect pollutants or other chemicals.

Figure 2(b) illustrates the transmittance of Ag-doped zinc oxide NPs synthesized hydrothermally. The material showed a permanent increase in transmittance in the UV area of the plot, showing electron transfer from the UV light spectrum. As the wavelength increases from 300 to 1100 nm, the transmittance of nanoparticles also increases. Zinc oxide doped with 0.3 mol of silver showed the highest transmittance in both spectral regions, whereas zinc oxide doped with 0.1 mol of silver exhibited the lowest absorbance. The material made with 0.3 mol of silver shows moderate transmittance compared to other materials (Mohan *et al.*, 2020; Khudiar, Mutlak and Nayef, 2021; Strachowski *et al.*, 2022; Zhou *et al.*, 2023). The materials' transmittance matches the transmittance mentioned in the literature. The addition of silver alters the optical properties of ZnO. The introduction of silver allows for the formation of extra energy levels in the bandgap, altering the behavior of light. Localized surface plasmon resonance in silver nanoparticles can boost light absorption in certain wavelengths and possibly decrease transmittance. Strong absorption is showed by peaks in the spectrum, which correlate with reduced transmittance. The wavelength usually affects the variation in transmittance. In the visible range, ZnO has good transmittance, but when silver is added, it changes and starts absorbing. Increased silver concentrations cause more scattering and absorption, resulting in reduced transmittance. The interaction between light and nanoparticles depends on their dimensions and morphology. The presence of smaller nanoparticles results in increased light scattering, which can influence transmittance. Transparent conductive materials like touch screens and solar cells can utilize silver-doped zinc oxide nanoparticles because of their high transmittance. Optical coatings can utilize the transmittance properties for specific light filtering in sensors and devices.

The reflectance of silver-doped zinc oxide nanoparticles, synthesized via a hydrothermal approach, is depicted in Figure 2 (c). The material displayed a permanent peak in reflectance in the visible region of the plot, suggesting a reflection of electrons in the UV light spectrum. Reflectance shows a decrease as the wavelength increases from 300 to 1100 nm. Zinc oxide doped with 0.1 mol of silver showed the highest reflectance in both spectral regions, whereas zinc oxide doped with 0.2 mol of silver had the lowest reflectance. Among all the materials, the material made with 0.3 mol of silver shows a moderate reflectance. The addition of silver to ZnO modifies its electronic structure and optical properties, resulting in varying reflectance levels depending on the size and concentration of the silver nanoparticles (Malik *et al.*, 2015; Król *et al.*, 2017; Lakshmipriya and Gopinath, 2020; Mohan *et al.*, 2020; Strachowski *et al.*, 2022). The presence of silver nanoparticles causes a localized surface plasmon resonance, influencing the way light is scattered and absorbed, affecting the reflectance spectrum. Variations in reflectance are commonly observed across different wavelengths, showing specific electronic transitions or plasmonic effects through distinct peaks or dips. Higher levels of silver can cause enhanced scattering, leading to increased reflectance in certain wavelength ranges. Light reflection is influenced by the roughness of nanoparticle surfaces, causing rough surfaces to exhibit higher scattering and reflectance. Optical coatings for mirrors and reflective surfaces benefit from the use of silver-doped zinc oxide nanoparticles for controlled reflectance. Enhanced light trapping and improved overall efficiency can be achieved in solar cells by optimizing reflectance.

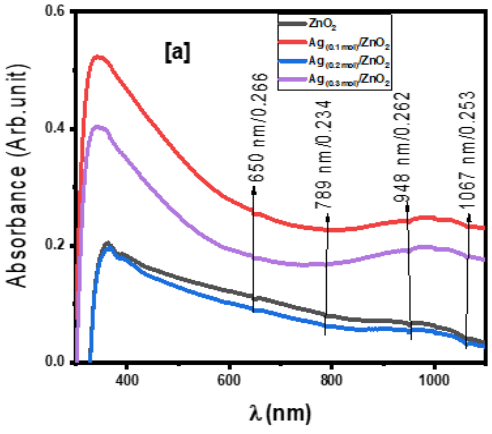

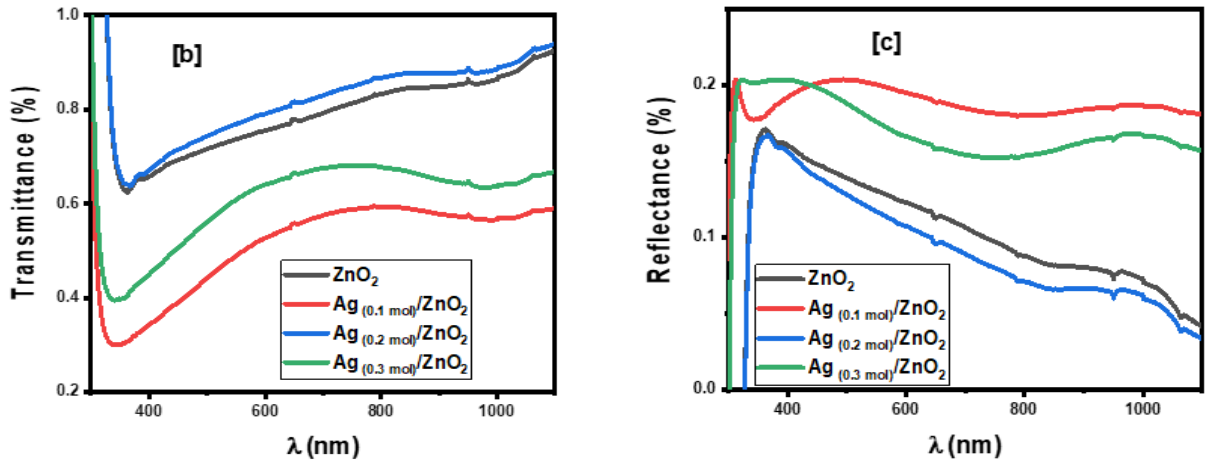

Figure 2: [a]-absorbance, [b]-transmittance, and [c]-reflectance of Ag-doped zinc oxide NPs

B. Bandgap Energy of Ag-doped zinc oxide NPs

The energy bandgap is the difference in energies between the valence band (the band filled with electrons at the highest energy level) and the conduction band (the band with the lowest energy where electrons can move freely). The material's electrical conductivity and optical absorption characteristics are determined by it. At room temperature, ZnO has a direct bandgap of approximately 3.37 eV (Mohan *et al.*, 2020; Khudiar, Mutlak and Nayef, 2021; Strachowski *et al.*, 2022; Zhou *et al.*, 2023), enabling efficient absorption of UV light. The energy bandgap of ZnO_2 in this study is 2.19 eV in Figure 3, which differs from the theoretical bandgap of ZnO. Introducing silver into ZnO can create additional energy levels, altering the electronic structure. The effective bandgap energy can be altered. The bandgap energy decreases from 1.50, 1.39, and 1.29 eV when silver is doped, enabling electron transitions at lower energy levels through the creation of defect states or interaction with ZnO. Using Tauc's equation, the absorption coefficient was related to the photon energy to estimate the bandgap energy. A change in bandgap energy is showed by a shift in the absorption edge. The bandgap decreases in energy because of the concentration of silver and the size of the nanoparticles. Increasing silver concentrations result in more pronounced changes in the band structure, which decrease the bandgap energy to 1.29 eV. The bandgap is influenced by the quantum size effect (Malik *et al.*, 2015; Król *et al.*, 2017; Lakshmipriya and Gopinath, 2020; Mohan *et al.*, 2020; Strachowski *et al.*, 2022). The bandgap energies of smaller nanoparticles are larger because of quantum confinement. Silver-doped zinc oxide nanoparticles with a smaller bandgap can absorb visible light, boosting their photocatalytic activity in water splitting and pollutant degradation. Optimizing the bandgap energy enhances sensor sensitivity to specific light wavelengths.

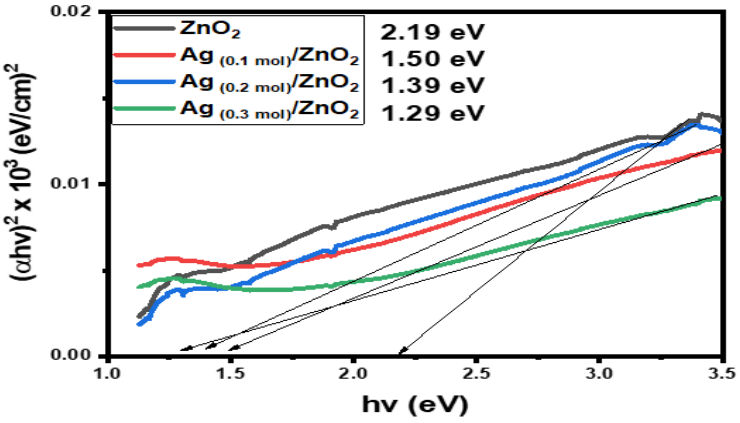

Figure 3: Bandgap energy of Ag-doped zinc oxide NPs

C. XRD study of Ag-doped zinc oxide NPs

Figure 4 illustrates the phase analysis conducted to study the material's structural analysis. The XRD patterns of ZnO and Ag-doped zinc oxide NPs show a similar hexagonal structure. At a 2θ angle of 44.863°, the material exhibited a diffraction peak at (101). The hexagonal phase exhibited well-defined diffraction peaks at specific 2θ angles. The sizes of the material's crystallites are depicted in Table 1. Scherrer's equation was used to determine the crystallite size, lattice constants, inter-planar distance, and dislocation densities, as shown in equations 1 to 3. The shift in peak intensity of Ag-doped zinc oxide NPs results from introducing silver ions into the ZnO lattices. The ionic radius of silver ions (Ag^{+}) differs from that of zinc ions (Zn^{2+}). Adding Ag^{+} for Zn^{2+} in the ZnO lattice alters the lattice parameters, causing a shift in XRD peaks. Introducing silver into the ZnO lattice causes strain because of disparities in size and charge between the dopant ions. Peak shifts in the XRD pattern can be attributed to this strain. Doping alters the crystallinity of ZnO nanoparticles. Increased crystallinity results in decreased peak intensity, while changes in phase cause peak positions to shift (Mohan *et al.*, 2020). The XRD pattern undergoes more noticeable shifts and changes when there are higher concentrations of silver ion, because of increased interactions between the dopant and the host lattice. The structural properties in Table 1, such as lattice constant (a), crystallite size (D), and d-spacing (d) were determined using Scherer's mathematical relation and equations (1-3) (Agnes C. Nkele *et al.*, 2020; Rufus *et al.*, 2023; Samuel *et al.*, 2023; Samuel, James 2023; Sarwar *et al.*, 2023; Akpu *et al.*, 2023; Akpu, Sylvanus and Nwaokorongwu, 2023; Josephine, Ikponmwosa 2023; Kufre I Udofia *et al.*, 2023; Kufre I. Udofia *et al.*, 2023; Uchechukwu *et al.*, 2024;). The size of crystallites clearly increases with the concentration of silver ions, as shown in Table 1. Initially, the nucleation rate rises as the concentration of silver ions increases, resulting in the formation of more nuclei. As the concentration rises, the nuclei do not form new ones but grow larger, resulting in larger crystallites. Increased silver ion concentrations result in lower surface energy, promoting the growth of bigger crystallites. Larger particles are stabilized because of the presence of silver, which changes the energetics of the system. Silver ions affect the growth kinetics of ZnO crystals. This alters the mechanisms of growth, encouraging the development of larger crystals instead of smaller ones. Increased silver concentrations during synthesis result in higher local temperatures or changes in the chemical environment, facilitating the growth of larger crystallites. The ionic radius of silver ions (Ag^{+}) is smaller than zinc ions (Zn^{2+}) (Mohan *et al.*, 2020). The crystal structure contracts and the d-spacing between crystal planes decreases when Ag^{+} ions are substituted for Zn^{2+} ions. The inclusion of silver in ZnO lattices causes strain due to size differences. The crystal structure of this strain adjusts to accommodate silver, resulting in a compression of the lattice and a decrease in d-spacing. The ZnO lattice incorporates silver ions to form a solid solution at higher silver concentrations. Because of this incorporation, atoms became arranged in a more condensed manner, causing a decrease in d-spacing. The band structure of the ZnO nanoparticles is affected by silver. The electronic environment changes influence the atomic arrangement in the lattice, which could cause a decrease in distances between atomic planes. The addition of silver (Ag) ions causes a distortion in the crystal structure of ZnO. The distortion results in a decrease in the intensity of certain diffraction peaks, especially those related to the ZnO phase. The entry of Ag ions into the ZnO lattice causes a shift in the lattice parameters, altering the diffraction peaks. Peaks may appear to shift out of range or merge with nearby peaks, affecting their detection. Introducing Ag doping causes lattice strain as a result of the difference in ionic radii between Zn^{2+} and Ag^{+} (Malik *et al.*, 2015; Zhou *et al.*, 2023). As the crystal structure becomes more disordered, this strain results in the broadening of peaks and, in certain cases, their complete disappearance.

$$D = {k\lambda}/{\beta\cos\theta} \quad (1)$$

$$d = {\lambda}/{2\sin\theta} \quad (2)$$

$$a = d\sqrt{h^2 + k^2 + l^2} \quad (3)$$

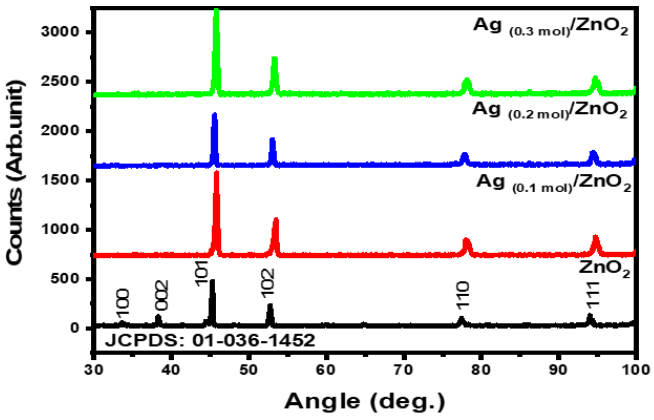

Figure 4: XRD pattern of Ag doped zinc oxide NPs

Table 1: Structural parameters of Ag doped zinc oxide NPs

Materials	Angle (deg.)	d-spacing (Å)	Latt. Const. (Å)	FWHM β	hkl	D (nm)	Dislocation density lines/m^2 (10^{15})
ZnO	33.704	2.6588	4.6052	0.5116	100	0.2834	3.7927
	38.238	2.3533	4.7067	0.5119	002	0.2869	3.7008
	44.863	2.0200	4.0400	0.5123	101	0.2930	3.5475
	52.518	1.7422	3.8957	0.5125	102	0.3019	3.3419
	77.496	1.2315	3.0166	0.5127	110	0.3470	2.5294
	94.312	1.0513	2.9735	0.5129	111	0.3979	1.9244
Ag $_{(0.1)}$/ZnO	45.755	1.9827	3.4341	0.2885	101	0.5220	1.1177
	53.533	1.7115	3.4231	0.2882	102	0.5392	1.0475
	78.249	1.2215	2.4431	0.2879	110	0.6213	7.8917
	95.019	1.0453	2.3374	0.2877	111	0.7141	5.9745
Ag $_{(0.2)}$/ZnO	45.755	1.9827	3.4341	0.2685	101	0.5609	9.6814
	53.533	1.7115	3.4231	0.2682	102	0.5794	9.0716
	78.249	1.2215	2.4431	0.2679	110	0.6677	6.8333
	95.019	1.0453	2.3374	0.2677	111	0.7674	5.1727
Ag $_{(0.3)}$/ZnO	45.755	1.9827	3.4341	0.2695	101	0.5588	9.6814
	53.533	1.7115	3.4231	0.2692	102	0.5773	9.0716
	78.249	1.2215	2.4431	0.2689	110	0.6652	6.8333
	95.019	1.0453	2.3374	0.2687	111	0.7646	5.1727

D. FTIR study of Ag doped zinc oxide NPs

FTIR spectroscopy is used to identify functional groups, evaluate surface chemistry, and study interactions between silver and zinc oxide in nanoparticles. This method aids in the characterization of material properties and verifying successful silver doping. In the FTIR spectrum, distinct absorption bands typically show Zn-O stretching vibrations, typically falling within the range of 400 to 750 cm^{-1}. Introducing silver doping creates new vibrational modes and shifts existing peaks, showing alterations in the local environment surrounding the ZnO lattice. The presence of hydroxyl groups (–OH), carbonates, or other organic residues from synthesis can cause additional peaks to appear. Figure 5 illustrates the FTIR measurements taken from a range of 4000 to 400 cm^{-1}. Bands in this range occur because of the vibration of ions in the crystal lattice (Bulcha *et al.*, 2021). The string band around 3459 cm^{-1} in all nanoparticles suggests OH stretching vibration. The oscillation of water molecules is a potential explanation (Malik *et al.*, 2015; Król *et al.*, 2017; Lakshmipriya and Gopinath, 2020; Mohan *et al.*, 2020; Strachowski *et al.*, 2022). For the Ag $_{(0.1)}$/ZnO2 nanoparticles, the wave number shift is towards the higher side and the intensity is higher. In Ag $_{(0.2)}$/ZnO, the band was present, but in Ag $_{(0.3)}$/ZnO, it was broader. The water content and energy levels have the potential to rise. The band expansion in silver-doped zinc oxide might be associated with a decrease in particle size. The nanoparticles of silver doped zinc oxide show a shift in wave number during observation. Nanoparticles display the 2924 cm^{-1} band associated with –CH_2 vibration. The band observed at 1450 cm^{-1} shows a C=O functional group. The peak intensity in Ag $_{(0.1)}$/ZnO is observed to be stronger. The band at 1150 cm^{-1} represents symmetric C–O stretching. This band is shifted to a higher wave number side for Ag $_{(0.2)}$/ZnO and Ag $_{(0.2)}$/ZnO, and for Ag $_{(0.3)}$/ZnO it is also shifted to a higher wave number side. The alteration in the Zn-O vibration peaks shows modifications in bond strength or the creation of new phases caused by the addition of silver. The variation in peak intensity shows the concentration of silver or the effectiveness. Analyzing the FTIR spectrum of pure ZnO and Ag-doped zinc oxide Nps reveals the impact of silver doping on the material's structure and chemistry. The addition of silver (Ag) changes the surrounding environment of the ZnO lattice. The change affects the vibrational modes of ZnO, causing systematic shifts in FTIR peaks with varying Ag concentration. Introducing Ag doping result in distortion within the ZnO crystal lattice. The distortion affects bond lengths and angles, altering vibrational mode energies and causing consistent shifts in the FTIR spectra. The electronic structure and charge carrier dynamics in ZnO be altered by introducing Ag. The phonon interactions affected, causing shifts in the observed vibrational frequencies in FTIR. The formation of new phases or compounds within the ZnO lattice depends on the concentration of Ag. The unique vibrational characteristics of these new phases can affect the FTIR spectrum, resulting in consistent shifts among various samples. The interaction between Ag and ZnO result in creating Ag-O bonds, causing shifts or new vibrational modes in FTIR peaks (Malik *et al.*, 2015; Mohan *et al.*, 2020; Strachowski *et al.*, 2022; Zhou *et al.*, 2023). The shifts in FTIR peaks suggest structural and electronic changes caused by Ag doping in ZnO.

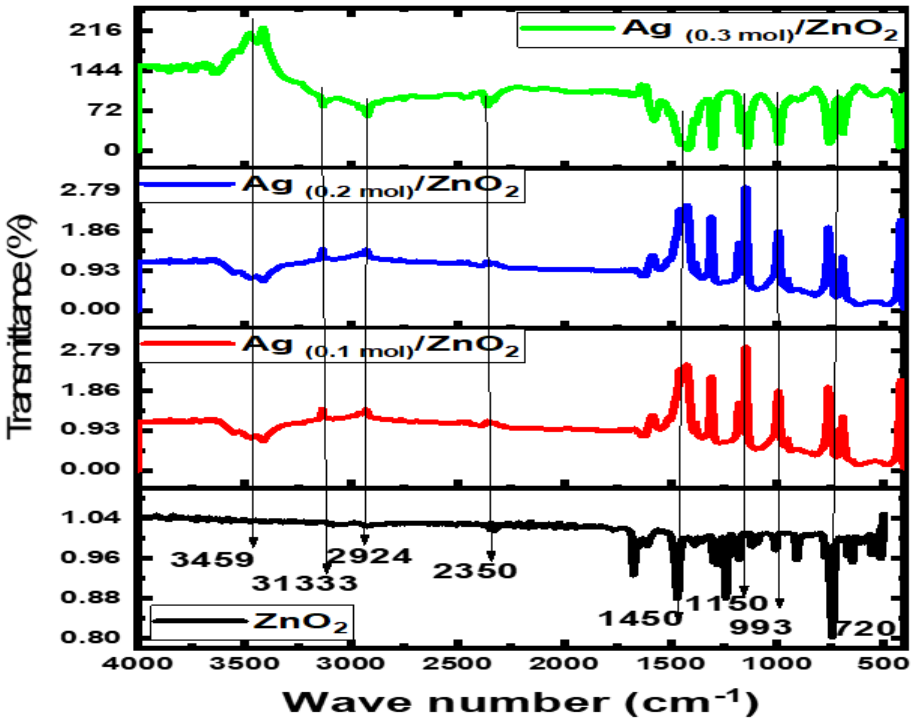

Figure 5: FTIR spectrum of Ag doped zinc oxide NPs

E. Surface morphological study of Ag doped zinc oxide NPs

The crystallization of ZnO commonly results in a hexagonal wurtzite structure, which has a significant surface area. The polar surface formed by zinc and oxygen atoms influences their reactivity and interactions. Nanoparticles produced through the hydrothermal method can take on different shapes, including nanorods, nanoplates, or flower-like structures. The shapes of these morphologies were determined by factors like temperature and silver precursor concentration. The electronic properties of ZnO nanoparticles are influenced by surface defects like vacancies or interstitials. The defects also function as active sites where chemical reactions take place. The surface structure of zinc oxide and Ag doped zinc oxide NPs synthesized using hydrothermal method is shown in Figure 6. The morphology displays the agglomeration of cluster nanoparticles resulting from the synthesis approach. Altering the reaction parameters allowed for the formation of various shapes with the silver dopant. The structural properties of the synthesized nanoparticles are influenced by the silver dopant. The micrograph of the zinc oxide surface shows a flower-like structure, non-spherical granular shape, and nanorod-like structure. Introducing silver into the ZnO lattice leads to a transformation in morphology, resulting in the formation of nano-sheets with agglomeration because of the presence of the silver dopant. The surface morphology of ZnO nanoparticles changes because of the presence of silver. The dispersion of silver ions in the ZnO matrix alters surface area and reactivity (Malik *et al.*, 2015; Król *et al.*, 2017; Lakshmipriya and Gopinath, 2020; Mohan *et al.*, 2020; Strachowski *et al.*, 2022). The addition of silver to ZnO improves its photocatalytic activity through synergistic effects (Rahmah *et al.*, 2023). The silver acts as a sink for electrons, enhancing charge separation and decreasing recombination rates. The addition of silver nanoparticles boosts light absorption and enhances the photocatalytic efficiency of silver-doped zinc oxide nanoparticles in visible light through surface plasmon resonance. The hydrothermal synthesis method produces ZnO and Ag doped zinc oxide NPs with distinct crystal structures, various morphologies, and surface defects. Silver (Ag) atoms have a smaller size compared to zinc (Zn) atoms. When Ag is added to the ZnO structure, it can either fill interstitial spaces or replace Zn atoms. The rearrangement of the lattice structure caused by the addition affected the overall porosity. The addition of Ag modifies the nucleation and growth dynamics of ZnO crystals. The

presence of Ag doping leads to the creation of larger pores because of altered crystallization patterns. Introducing Ag leads to the creation of new phases that fill the ZnO lattice, effectively decreasing pore size. These changes affect the distribution and connectivity of the pores as well. Doping modifies the surface energy of ZnO, affecting the development and expansion of pores (Malik *et al.*, 2015; Mohan *et al.*, 2020; Strachowski *et al.*, 2022; Zhou *et al.*, 2023). The addition of 0.3 mol of silver through doping enhances the functionality of zinc oxide nanoparticles, making them highly useful in applications such as photocatalysis, sensors, and antimicrobial agents (Venkatasubramanian and Sundaraj, 2014; Rahmah *et al.*, 2023). Figure 7 displays the EDXs spectrum of ZnO and Ag doped zinc oxide NPs. The spectrum shows all the elements in ZnO and Ag doped zinc oxide NPs. A prominent peak signals the presence of zinc. The oxygen peak is part of the structure of zinc oxide. Silver peaks show successful doping of silver into the zinc oxide lattice. The hexagonal wurtzite structure of zinc oxide (ZnO) consists mainly of zinc atoms. When ZnO is doped with Ag, it either replaces Zn atoms or occupies interstitial sites. Still, the crystal framework mostly consists of ZnO, resulting in prominent zinc-related peaks in the spectrum. The concentration of Ag is relatively small in comparison to Zn, making the zinc contribution more significant than the FTIR and XRD peaks. The reason is that most of the lattice is still made up of ZnO, making the zinc-related vibrations or peaks more noticeable. The presence of Ag affects the electronic properties of ZnO, but the dominant vibrational modes related to zinc remain unchanged. The fundamental vibrational modes of ZnO are unlikely to be significantly changed by Ag doping and its electronic transitions. Ag as a dopant alters the band structure and introduces new electronic states, while the fundamental vibrational characteristics of the ZnO lattice remain largely unchanged (Malik *et al.*, 2015; Mohan *et al.*, 2020; Strachowski *et al.*, 2022; Zhou *et al.*, 2023). As a result, the peaks related to Zn will remain more noticeable. The zinc peak is predominantly observed in Ag-doped ZnO because of the ZnO structure, dopant concentration, and Ag-ZnO lattice interactions.

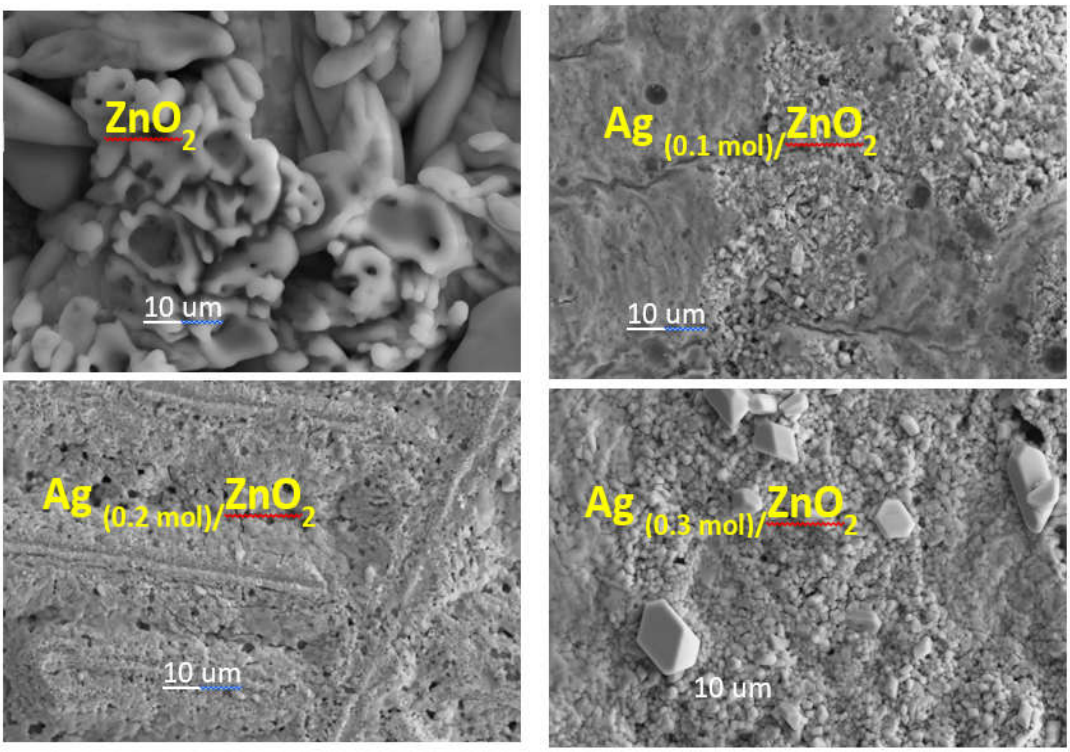

Figure 6: surface micrograph of silver doped zinc oxide nanoparticles

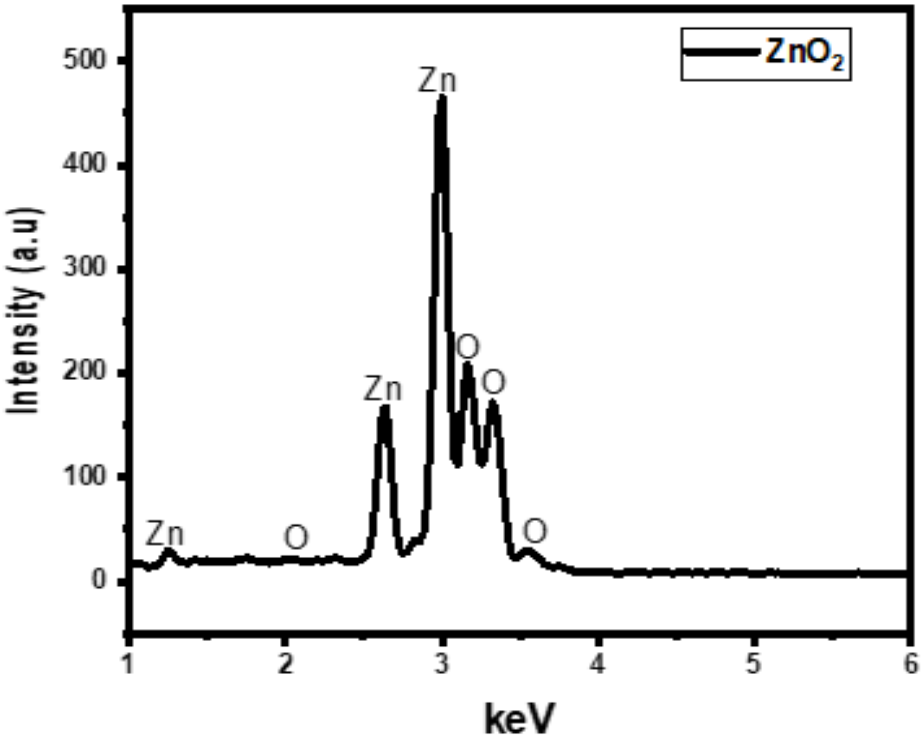

(a)

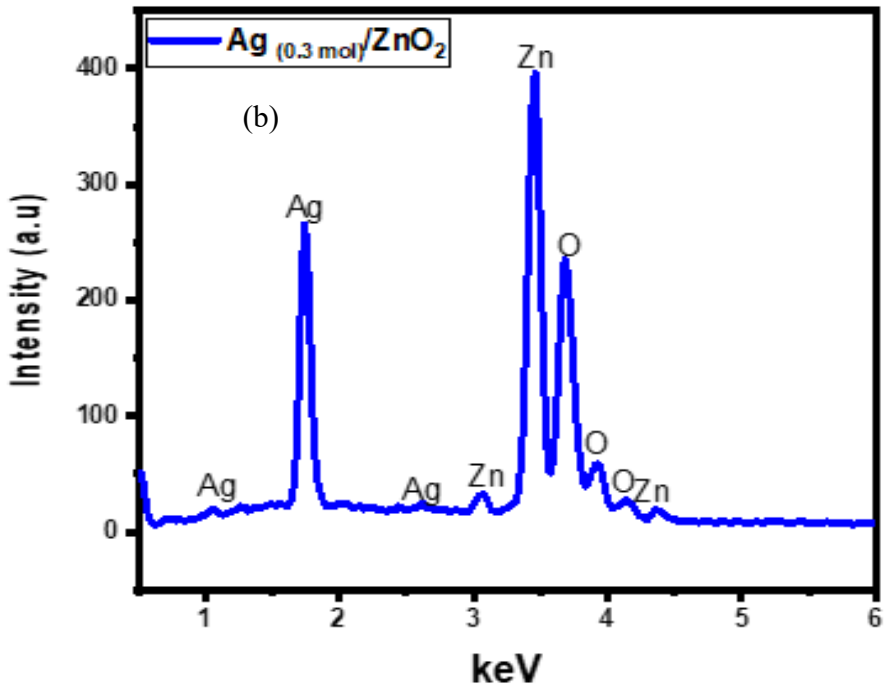

(b)

Figure 7: EDX spectrum of silver doped zinc oxide nanoparticles

V. CONCLUSIONS

The hydrothermal method was used to synthesize ZnO and Ag doped zinc oxide NPs. The hexagonal structure of ZnO and Ag doped zinc oxide NPs is reflected in their XRD patterns. The material showed a diffraction peak at (101) when measured at a 2theta angle of 44.863°. The hexagonal phase displayed distinct diffraction peaks at specific 2theta angles. Within the FTIR spectrum, Zn-O stretching vibrations are typically indicated by distinct absorption bands, usually ranging from 400 to 750 $cm^{-1.}$ Introducing silver doping results in the emergence of new vibrational modes and a shift in existing peaks, indicating changes in the local environment around the ZnO lattice. Nanoparticles exhibit a decrease in absorbance with increasing incident light wavelength from 300 to 1100 nm. The highest absorbance was recorded in zinc oxide doped with 0.1 mol of silver in both spectral regions, whereas the lowest absorbance was observed in zinc oxide doped with 0.2 mol of silver. In this study, the energy bandgap of ZnO_2 is measured at 2.19 eV, which deviates from the theoretical bandgap of ZnO. Introducing silver into ZnO leads to changes in the band structure because of the creation of additional energy levels. Introducing silver doping into ZnO lattice leads to a decrease in bandgap energy from 1.50, 1.39, and 1.29 eV, enabling electron transitions at lower energy levels because of the formation of defect states or interaction with ZnO. The hydrothermal synthesis of Ag-doped ZnO nanoparticles shows great promise for diverse applications because of their improved characteristics. By utilizing the hydrothermal process, one can achieve precise control over particle size, morphology, and doping levels, ultimately enhancing the nanoparticles' crystallinity and stability. The addition of silver alters both the optical and electronic properties, improving optical performance and making these nanoparticles ideal for environmental remediation and electronics applications. The hydrothermal method is effective for producing tailored Ag-doped ZnO nanoparticles, promising advancements in nanotechnology and material science.

AUTHOR CONTRIBUTIONS

E. O. Ojegu, R. A **Daniel-Umeri, E. C. Nwaokorongwu**: conceptualization, method development, and experimentation, **E. C. Nwaokorongwu and Nawal Alghamdi, I. L. Ikhioya**: writing the original draft. Modifying the initial draft, performing graphical design, and providing references. **Nawal Alghamdi and I. L. Ikhioya**: Conducting investigations and providing supervisory oversight.

REFERENCES

A.R. and M.I.T. (2022). 'synthesis of silver (ag) doped zinc oxide (zno) nanoparticles as efficientphotocatalytic activity for degradation methylene blue dye. Journal of Advanced Scientific Research, 13 (02), pp. 129–135.

Aravind, A.J., Kumar, M.K., Mukesh; Chandra R. (2013). Optical and magnetic properties of copper doped ZnO nanorods prepared by hydrothermal method. Journal of Materials Science: Materials in Electronics, 24 (1), pp. 106–112.

Bekele, B., Jule, L.T., Degefa, A.R., Shanmugam, L.P.D., Nagaprasad N. and Ramaswamy K. (2021). Synthesis of Zinc Oxide Nanoparticles by Hydrothermal Methods and Spectroscopic Investigation of Ultraviolet Radiation Protective Properties', Journal of Nanomaterials, 2021. 17 (12), pp. 1448–1459.

Chinwe, U.U., Anthony O. N.,, Joshua, C.E., Ikhioya, L.L., Odira, O.A.O. (2024). Investigating the influence of natural dye extracts from Ocimum gratissimum , Solanum melongena , Piper guineese , and their blend in the fabrication of perovskite solar cells', Hybrid Advances, 6(April), pp. 100198.

Dhoke, S.K. (2023). Synthesis of nano-ZnO by chemical method and its characterization. Results in Chemistry, 5 (January), pp. 100771.

Hashem, A.H. and El-Sayyad, G.S. (2023). Antimicrobial and anticancer activities of biosynthesized bimetallic silver-zinc oxide nanoparticles (Ag-ZnO NPs) using pomegranate peel extract', Biomass Conversion and Biorefinery [Preprint]. 15(11), pp. 1348–1359.

Ijeh R, Asarhasa P, Samson O. A, (2023). Results in Optics Influence of manganese molarity incorporation on manganese silver sulphide semiconductor material for photovoltaic applications', Results in Optics, 12 (February), pp. 100464.

J.N. Hasnidawani, H.N. Azlina, H. Norita, N.N. Bonnia, S. Ratim, E.S. Ali (2016). Synthesis of ZnO Nanostructures Using Sol-Gel Method', Procedia Chemistry, 19, pp. 211–216.

Josephine, E. N., Ikponmwosa, O. S., Alomayri, T. (2023). 'Enhanced physical properties of SnS/SnO semiconductor material', Asian Journal of Nanoscience and Materials, (3), pp. 199-212.

Khudiar, S.S., Mutlak, F.A.H. and Nayef, U.M. (2021). Synthesis of ZnO nanostructures by hydrothermal method deposited on porous silicon for photo-conversion application, Optik, 247 (No. 2):167903.

Król, A., Pomastowski, P., Rafińska, K, Railean-Plugaru, V., and Buszewski, B. (2017). Zinc oxide nanoparticles: Synthesis, antiseptic activity and toxicity mechanism, Advances in Colloid and Interface Science, 249, pp. 37–52.

Lakshmipriya, T. and Gopinath, S.C.B. (2020). Introduction to nanoparticles and analytical devices, Nanoparticles in Analytical and Medical Devices, 4 (01) pp. 1–29.

M. Chandrasekar, S. Panimalar, R. Uthrakumar, M. Kumar, M.E. Raja Saravanan, G. Gobi, P. Matheswaran, C. Inmozhi, K. Kaviya (2019). Preparation and characterization studies of pure and Li+doped ZnO nanoparticles for optoelectronicapplications, Materials Today: Proceedings, 36, pp. 228–231.

M. Jothibas; A. Muthuvel; K. Senthilkannan; V. Mohana (2019). Structural, optical and photocatatic activity of Ag doped ZnO nanoparticles obtained by sol-gel method, AIP Conference Proceedings, 2162.

Malik, John, (2015). ZnO Nanoparticles: Growth, Properties, and Applications Research. 2, pp. 23-45. https://scholar.smu.edu/ce.

N. I. Akpu, Cissan A. Sylvanus, Elizabeth C. Nwaokorongwu. Emmanuel O. Okechukwu, Laeticia U. Ugwu, Azubuike J. Ekpunobi (2023). Modulation of the physical properties of spray-deposited cobalt selenide nanofilm via yttrium doping for photovoltaic purposes . J. Mater. Environ. Sci., 2023, Volume 14, Issue 11, Page 1230-1244

N. I. Akpu, K. U. P. Okpechi, Elizabeth C. Nwaokorongwu, Julian C. Onwuzo, Lebe A. Nnanna, Ifeanyi I. C. Agbodike (2023). Impact of temperature difference on the features of spray deposited yttrium doped cobalt selenide (YCoSe) thin films for photovoltaic application, African Scientific Reports, 2, pp. 143-146.

P. M. Aneesh, Vanaja, K.A. and Jayaraj, M.K. (2007). Synthesis of ZnO nanoparticles by hydrothermal method', Nanophotonic Materials IV, 6639 (September 2007), pp. 66390J.

Primo, J. D., Bittencourt, C., Acosta, S., Colomer, J., Jaerger, S., Teixeira, V. C., & Anaissi, F. J. (2020) 'Synthesis of Zinc Oxide Nanoparticles by Ecofriendly Routes: Adsorbent for Copper Removal From Wastewater', Frontiers in Chemistry, 8. pp. 45-49.

Rahmah M. I, Majdi H. S. A, Waleed K, Rasn M. J, Jasim, Hadi H, Majid S. A, Roonak A. S. A. Rashid T. M. (2023).'Synthesis of ZnO/Ag-doped C/N heterostructure for photocatalytic application', International Journal of Modern Physics B, 37 (24).

Saima M, Shazia N, Sania M. A, Farooq S, Farida B, Muhammad I, Mohammed A. A, ArifaNouroz, Nadra N, Zarmina A. K, and Parveen A. (2023). Synthesis and Characterization of ZnO Nanoparticles Derived from Biomass (Sisymbrium Irio) and Assessment of Potential Anticancer Activity, ACS Omega, 8 (18), pp. 15920–15931.

Sakhi G. Sarwar, Ikhioya, I.L, Shahbaz Afzal, Ishaq Ahmad, (2023). Supercapitance performance evaluation of MXene/Graphene/NiO composite electrode via in situ precipitation technique, Hybrid Advances, 4, pp. 100105.

Samuel, S. O., James, F. E., JT, Z., EP, O., Ekpekpo, A., (2024). Effect of dopant on the energy bandgap on strontium sulphide doped silver for optoelectronic application. Materials Research Innovations, 28(1), 8-18.

Samuel, S. O., Timothy, Z. J., Ojoba, C. K., (2023). Temperature's Impact on the Physical Properties of Rare Earth Element Doped SrS for Optoelectronic Use. Journal of Engineering in Industrial Research, 4 (3), 147-156.

Sonima M, Mini V, Arun A, and Reka U (2020). Hydrothermal synthesis and characterization of Zinc Oxide nanoparticles of various shapes under different reaction conditions, Nano Express, 1 (3) pp. 456-467.

Strachowski, T.; Baran, M.; Małek, M.; Kosturek, R.; Grzanka, E.; Mizeracki, J.; Romanowska, A.; Marynowicz, S. (2022). Hydrothermal Synthesis of Zinc Oxide Nanoparticles Using Different Chemical Reaction Stimulation Methods and Their Influence on Process Kinetics. Materials, 15, 7661.

Udofia, K. I, Ikhioya, I.L., Donald N. Okoli, Azubike J. Ekpunobi, (2023). Impact of doping on the physical properties of PbSe chalcogenide material for photovoltaic application, Asian Journal of Nanoscience and Materials, 6(2), pp. 135–147.

Venkatasubramanian, K. and Sundaraj, S. (2014). Antibacterial activity of Zinc Oxide and Ag doped Zinc Oxide Nanoparticles against E . coli, 3(9), pp. 40–44.

Widiyandari H, Pratama E. D, Parasdila H, Suryana R, Arutanti O, Astuti Y. (2023). Synthesis of ZnO-Cdots nanoflower by hydrothermal method for antibacterial agent and dye photodegradation catalyst, Results in Materials, 20(November), pp. 100491.

Zhou, X.-Q.; Hayat, Z.; Zhang, D.-D.; Li, M.-Y.; Hu, S.; Wu, Q.; Cao, Y.-F.; Yuan, Y. (2023). Zinc Oxide Nanoparticles: Synthesis, Characterization, Modification, and Applications in Food and Agriculture. Processes 2023, 11(4), 1193